encit 2020

ABCM
Associação Brasileira de Engenharia e Ciências Mecânicas

18th Brazilian Congress of Thermal Sciences and Engineering
November 16–20, 2020 (Online)

ENC-2020-0810
ATTENUATION COEFFICIENT ESTIMATION IN THERMAL ABLATION PROCEDURES

Ingrid M. Ventura[1]
Luiz A. S. Abreu[2]
Polytechnic Institute, Rio de Janeiro State University (IPRJ/UERJ), Nova Friburgo, RJ, Brazil
[1]imventura@iprj.uerj.br; [2]luiz.abreu@iprj.uerj.br

Bruna R. Loiola
Military Institute of Engineering (IME), Mechanical Engineering Department, Rio de Janeiro - 22290-270, Brazil
bruna.loiola@ime.eb.br

Abstract. *Laser ablation procedures have been increased in medical applications due to be less invasive than open surgeries. In this type of procedure, the optical properties due the interaction between laser and tissue are of great relevance. Thus, the goal of this study is to estimate the attenuation coefficient related to a laser heat source used in thermal ablation procedures. The classical bioheat equation was applied considering a human skin heated by a continuous laser. The solution of the direct problem was solved using generalized integral transform technique to obtain the simulated temperature measurements. The numerical solution was verified against others direct solution methodologies. The inverse analysis was obtained with Markov Chain Monte Carlo method performed with Metropolis-Hastings algorithm. The comparison between direct approach solutions shows an excellent agreement and the attenuation coefficient is accurately estimated.*

Keywords: *optical properties, attenuation coefficient, bioheat transfer, inverse analysis*

1. INTRODUCTION

Thermal therapy has been used in several nations and countries throughout history, since the use of thermal baths in ancient roman civilization (Chato, 1992; Habash *et al.*, 2006), until wound cauterization in battles. Recently, due to the scientific and technological development, thermal ablation therapy has become more reliable and widely applied in complex treatments such as cancer treatments, cardiac and ophthalmologic surgeries. The effectiveness of these procedures is tied to the accuracy of knowledge about it. Therefore, it is important to have the correct information about the treatment conditions and their interaction with the human body (Habash *et al.*, 2006; Loiola *et al.*, 2020b).

In thermal therapy, a specific level of temperature is applied during a period of time. When low temperature is applied in a biological tissue and the time of application could be extended, it is characterized as diathermia or hyperthermia treatment. Instead, in thermal ablation therapies, the high temperature levels require a short time of process duration (Habash *et al.*, 2006). In all these treatments, there are certain properties that must be known, as the physical properties which can be measured using empirical or indirect methods.

Thermal ablation treatments use an external energy source, usually lasers, radiofrequency, or ultrasound, to achieve the desired temperatures in a biological tissue (Diller, 2010; Habash *et al.*, 2006; Loiola *et al.*, 2020b). In order to provide an effective result using lasers to heat a specific tissue, it is important to determine the tissue optical properties: the absorption and scattering coefficients, the scattering anisotropy, the scattering phase function and the effective attenuation coefficient. Usually, the measurements of these parameters are made with ex vivo samples or applying in vivo techniques and experimental measurements of light reflectance and transmittance. Also, transient temperature measurements could be used to determine these properties indirectly (Jacques and Prahl, 1987a; Jacques *et al.*, 1987b; Kim and Wilson, 2010; Nicolaides *et al.*, 2001; Prahl *et al.*, 1992; Welch, 1984; Welch *et al.*, 2010).

Jacques and Prahl (1987a), measured the reflectance and transmittance of an incident laser light in a skin of mice to define indirectly the viable optical properties. Besides that, Nicolaides *et al.* (2001), made an extended work, including theoretical, experimental, and computational analysis to estimate the optical scattering and absorption coefficients. In this kind of researches, a mathematical model needs to be defined to reach the optical properties using the indirect measurements (Jacques and Prahl, 1987a; Kim and Wilson, 2010; Nicolaides *et al.*, 2001). In the present work, the human skin properties (Cooper and Trezek, 1971) together with synthetic temperature measurements will be used to estimate the effective attenuation coefficient. The classical bioheat transfer equation proposed by Harry H. Pennes in 1948 will

be adapted to model mathematically a biological tissue heated by a continuous laser during the ablation clinical process (without material removal). The generalized integral transform technique (GITT) is applied in the direct solution and a Bayesian framework is then used to estimate the attenuation coefficient related to the interaction between the external laser source and the irradiated tissue in the inverse problem. A Markov Chain Monte Carlo (MCMC) method is applied using Metropolis-Hastings (M-H) algorithm considering simulated temperature measurements.

2. PHYSICAL PROBLEM AND MATHEMATICAL FORMULATION

In this present research, a two-dimensional geometry in cylindrical coordinates with an axisymmetric in z is considered to describe the biological tissue under study. The clinical ablation is handled by the classical equation for bioheat transfer (Pennes, 1948), presented in Eq. (1), where $T(r,z,t)$ is the temperature of the tissue varying according to the spatial coordinates r and z and the time t, for $t > 0$.

$$\rho c_p \frac{\partial T(r,z,t)}{\partial t} = k\left[\frac{1}{r}\frac{\partial T(r,z,t)}{\partial r} + \frac{\partial^2 T(r,z,t)}{\partial r^2} + \frac{\partial^2 T(r,z,t)}{\partial z^2}\right] + Q(r,z,t), \quad in\ \ 0 < r < R,\ 0 < z < H \tag{1}$$

The initial and boundary conditions are given by Eq. (2)-(6).

$$T(r,z,t) = Tb, \quad in\ \ 0 < r < R,\ 0 < z < H \quad for\ \ t = 0 \tag{2}$$

$$\frac{\partial T(r,z,t)}{\partial r} = 0, \quad in\ \ r = 0,\ 0 < z < H \quad for\ \ t > 0 \tag{3}$$

$$T(r,z,t) = Tb, \quad in\ \ r = R,\ 0 < z < H \quad for\ \ t > 0 \tag{4}$$

$$T(r,z,t) = Tb, \quad in\ \ 0 < r < R,\ z = 0 \quad for\ \ t > 0 \tag{5}$$

$$-k\frac{\partial T(r,z,t)}{\partial z} = h_\infty[T(r,z,t) - T_\infty], \quad in\ \ 0 < r < R,\ z = H \quad for\ \ t > 0 \tag{6}$$

In these equations ρ, c_p and k are, respectively, density, specific heat, and thermal conductivity associated to the biological tissue. The parameter h_∞ is the heat transfer coefficient considering convection and linearized radiation at the heating surface of the tissue, T_∞ is the temperature in the medium, T_b is the arterial blood temperature and Q refers to the heat source, described in Eq. (7).

$$Q(r,z,t) = \rho_b c_b w_b[T_b - T(r,z,t)] + Q_m + Q_l(r,z) \tag{7}$$

The quantities ρ_b and c_b are the density and the specific heat of the arterial blood, respectively. The tissue metabolic term is denoted by Q_m while the tissue perfusion coefficient is indicated by w_b. The laser heat source, obtained from Eq. (8), is given by Q_l applied in $z = H$ and it is modeled by the Beer-Lambert's law as a Gaussian beam (Loiola *et al.*, 2018, 2020a; Welch *et al.*, 2010).

$$Q_l(r,z) = \mu_{eff}\varphi_0 exp[-\mu_{eff}(H - z)]exp\left(\frac{-r^2}{2\sigma^2}\right) \tag{8}$$

The laser beam radius is defined as 2σ, μ_{eff} is the effective attenuation coefficient and $\varphi_0 = P/(2\pi\sigma^2)$ is the laser irradiance, in which P is the laser power. The coefficient μ_{eff} is related directly with the phenomenon of light absorption and scattering and describes the attenuation of light in a tissue considering the distance between the source and the position of interest (Welch *et al.*, 2010).

3. DIRECT (FORWARD) PROBLEM

In the direct problem, the parameters are known, the temperature field are computed and a linear filter in z, given in Eq. (9), is applied to hasten the convergence of the solution. This filter splits the mathematical model into a filter problem and a filtered problem.

$$T(r,z,t) = T_1(z) + T_2(r,z,t) \tag{9}$$

The filter problem is expressed in Eq. (10)-(12).

$$\frac{d^2 T_1(z)}{dz^2} = 0, \quad in\ \ 0 < z < H \tag{10}$$

$$T_1(z) = T_b, \quad in\ \ z = 0 \tag{11}$$

$$\frac{dT_1(z)}{dz} + \frac{h_\infty}{k} T_1(z) = \frac{h_\infty T_\infty}{k}, \quad in \;\; z = H \tag{12}$$

Equations (13)-(18) define the filtered problem under study, with $\alpha = k/(\rho c_p)$.

$$\frac{1}{\alpha}\frac{\partial T_2(r,z,t)}{\partial t} - \frac{\partial^2 T_2(r,z,t)}{\partial z^2} = \frac{1}{r}\frac{\partial T_2(r,z,t)}{\partial r} + \frac{\partial^2 T_2(r,z,t)}{\partial r^2} + \frac{Q(r,z,t)}{k}, \quad in \;\; 0 < r < R, \; 0 < z < H \tag{13}$$

$$T_2(r,z,t) = T_b - T_1(z), \quad in \;\; 0 < r < R, \; 0 < z < H \quad for \;\; t = 0 \tag{14}$$

$$\frac{\partial T_2(r,z,t)}{\partial r} = 0, \quad in \;\; r = 0, \; 0 < z < H \quad for \;\; t > 0 \tag{15}$$

$$T_2(r,z,t) = T_b - T_1(z), \quad in \;\; r = R, \; 0 < z < H \quad for \;\; t > 0 \tag{16}$$

$$T_2(r,z,t) = 0, \quad in \;\; 0 < r < R, \; z = 0 \quad for \;\; t > 0 \tag{17}$$

$$\frac{\partial T_2(r,z,t)}{\partial z} + \frac{h_\infty}{k} T_2(r,z,t) = 0, \quad in \;\; 0 < r < R, \; z = H \quad for \;\; t > 0 \tag{18}$$

The filter problem has analytical solution (Boyce and DiPrima, 2000). The filtered problem is solved by generalized integral transform technique with partial transformation scheme, using the integral transformation only over the coordinate z. The GITT is a hybrid technique which uses analytical and numerical approaches to solve non-transformable problems modeling by partial differential equation (PDE) (Cotta *et al.*, 2018; Abreu *et al.*, 2014). In this technique, the eigenvalue problem, or Sturm-Liouville problem, must be chosen. Considering the homogeneous version of Eq. (13)-(18) and $T_2(r,z,t) = \psi(z)\Gamma(r,t)$, the eigenvalue problem is defined as presented in Eq. (19)-(21).

$$\frac{d^2\psi(z)}{dz^2} + \beta^2 \psi(z) = 0, \quad in \;\; 0 < z < H \tag{19}$$

$$\psi(z) = 0, \quad in \;\; z = 0 \tag{20}$$

$$\frac{d\psi(z)}{dz} + \frac{h_\infty}{k}\psi(z) = 0, \quad in \;\; z = H \tag{21}$$

The solution of this problem gives the eigenfunction $\psi_i(z)$, the eigenvalues β_i and, consequently, the norm N_i, expressed in Eq. (22)-(24) (Ozisik, 1993).

$$\psi_i(z) = sin(\beta_i z), \tag{22}$$

$$\beta_i cot(\beta_i H) = -\frac{h_\infty}{k} \tag{23}$$

$$N_i = \frac{1}{\alpha}\int_0^H \psi_i^2(z)\, dz \tag{24}$$

Thus, Eq. (25) gives the normalized eigenfunction $\tilde{\psi}_i(z)$.

$$\tilde{\psi}_i(z) = \frac{sin(\beta_i z)}{\sqrt{N_i}} \tag{25}$$

Thereafter, the integral transform pair is defined. Eq. (26) and (27) give the transform and inversion formulae for the filtered problem to be solved (Cotta *et al.*, 2018).

$$\text{Transform: } \overline{T}_i(r,t) = \frac{1}{\alpha}\int_0^H \tilde{\psi}_i(z) T_2(r,z,t)\, dz \tag{26}$$

$$\text{Inversion: } T_2(r,z,t) = \sum_{i=1}^{\infty} \overline{T}_i(r,t)\tilde{\psi}_i(z) \tag{27}$$

From that point, the problem is integral transformed and a numerical method is applied to solve the system of coupled PDEs, Eq. (28)-(32), seeking the transformed potentials, $\overline{T}_i(r,t)$.

$$\frac{\partial \overline{T}_i(r,t)}{\partial t} + \beta_i^2 \alpha \overline{T}_i(r,t) = \overline{g}_i(r,t,\overline{\mathbf{T}}(r,t)), \quad i = 1,2,3,...,N \tag{28}$$

$$\overline{g}_i(r,t,\overline{\mathbf{T}}(r,t)) = \int_0^H \tilde{\psi}_i(z)\left[\frac{1}{r}\frac{\partial T_2(r,z,t)}{\partial r} + \frac{\partial^2 T_2(r,z,t)}{\partial r^2} + \frac{Q(r,z,t)}{k}\right] dz \tag{29}$$

$$\overline{T}_i(r,t) = \frac{1}{\alpha}\int_0^H \tilde{\psi}_i(z)(T_b - T_1(z))\, dz, \quad in\ \ 0 < r < R,\ \ for\ \ t = 0\ \ and\ \ i = 1,2,3,...,N \tag{30}$$

$$\frac{\partial \overline{T}_i(r,t)}{\partial r} = 0, \quad in\ \ r = 0,\ \ for\ \ t > 0\ \ and\ \ i = 1,2,3,...,N \tag{31}$$

$$\overline{T}_i(r,t) = \frac{1}{\alpha}\int_0^H \tilde{\psi}_i(z)(T_b - T_1(z))\, dz, \quad in\ \ r = R,\ \ for\ \ t > 0\ \ and\ \ i = 1,2,3,...,N \tag{32}$$

In this work, the transformed potentials was obtained numerically employing the built-in routine `NDSolve`, available in software Wolfram Mathematica® (Wolfram, 2020). Then, the solution for the potential $T_2(r,z,t)$ was reached using the inversion formula considering a number of terms N in the summation, large enough to achieve the convergence, according to the prescribed tolerance. So, the final solution for the biological tissue temperature is reached by applying Eq. (9).

4. INVERSE PROBLEM

In this study, the Bayesian inference is applied to estimate the parameters in the inverse problem. Bayesian inference is a statistical technique which allows combining the measurement information with known data about the parameters. Several methods to parameters and/or function estimation could be developed from this approach (Kaipio and Somersalo, 2004; Orlande, 2012; Rojczyk *et al.*, 2017). The Bayesian framework uses the Bayes'theorem, Eq. (33), in order to compute the posterior probability density function, $\pi(\mathbf{P}|\mathbf{Y})$ (Kaipio and Somersalo, 2004; Orlande, 2012; Orlande *et al.*, 2011; Ozisik and Orlande, 2000).

$$\pi(\mathbf{P}|\mathbf{Y}) = \frac{\pi(\mathbf{P})\pi(\mathbf{Y}|\mathbf{P})}{\pi(\mathbf{Y})}. \tag{33}$$

In Eq. (33), $\mathbf{P} = (P_1, P_2, ..., P_N)$ is the vector of parameters, $\mathbf{Y} = (Y_1, Y_2, ..., Y_D)$ is the vector of measurements that in this case is a vector of simulated temperature measurements, $\pi(\mathbf{P})$ is the prior density function, $\pi(\mathbf{Y}|\mathbf{P})$ is the likelihood function and $\pi(\mathbf{Y})$ is the marginal probability density of the measurements, which can be understand like a normalizing constant and generally has complex solution (Kaipio and Somersalo, 2004; Loiola *et al.*, 2020b; Abreu *et al.*, 2014; Orlande, 2012; Orlande *et al.*, 2011; Ozisik and Orlande, 2000; Rojczyk *et al.*, 2017).

In order to define the likelihood function, Eq. (34), the measurement errors are considered additive and independent of the parameters, furthermore, the errors are modeled as Gaussian random variables with zero means and known covariance matrix. In this function, $T(\mathbf{P})$ is the forward solution, D is the number of measurements and $\mathbf{W}$ is the covariance matrix.

$$\pi(\mathbf{Y}|\mathbf{P}) = (2\pi)^{-\frac{D}{2}}|\mathbf{W}|^{-\frac{1}{2}}\exp\left\{-\frac{1}{2}[\mathbf{Y} - T(\mathbf{P})]^T\mathbf{W}^{-1}[\mathbf{Y} - T(\mathbf{P})]\right\}. \tag{34}$$

The prior density function will be defined according to the available information about the parameters. In order to formulate this function, a Gaussian, a Rayleigh or a uniform distribution could be used. In this work, no prior information will be considered.

As mentioned above, the Markov Chain Monte Carlo will be applied in the solution of the inverse problem. The MCMC technique allows estimating the posterior probability density function using the Metropolis-Hastings algorithm, an acceptance-rejection sampling algorithm, which follows the steps (Loiola *et al.*, 2020b; Abreu *et al.*, 2014; Orlande, 2012; Orlande *et al.*, 2011; Ozisik and Orlande, 2000; Rojczyk *et al.*, 2017):

1. Start the chain at $\mathbf{P}^t$;
2. Sample a candidate $\mathbf{P}^*$ from $q(\mathbf{P}^*|\mathbf{P}^t)$, a proposal distribution;
3. Compute the acceptance probability of the candidate: $\alpha = min\left[1, \frac{\pi(\mathbf{P}^*|\mathbf{Y})q(\mathbf{P}^t|\mathbf{P}^*)}{\pi(\mathbf{P}^t|\mathbf{Y})q(\mathbf{P}^*|\mathbf{P}^t)}\right]$;
4. Calculate a random value U between 0 and 1;
5. If $\alpha \geq U$, accept $\mathbf{P}^*$ and set $\mathbf{P}^{t+1} = \mathbf{P}^*$ or reject $\mathbf{P}^*$ and make $\mathbf{P}^{t+1} = \mathbf{P}^t$;
6. Return to step 2 and repeat the process until the posterior distribution, $\pi(\mathbf{P}|\mathbf{Y})$, is represented adequately.

In the M-H algorithm, it is not necessary to compute $\pi(\mathbf{Y})$ because only the ratio between posterior probability density functions are considered. The application of the described technique has as result a sequence of samples $[\mathbf{P}^1, \mathbf{P}^2, \mathbf{P}^3, ..., \mathbf{P}^N]$. In this sequence, the values of $\mathbf{P}^i$ ideally converge to a region of equilibrium and the samples before the chain convergence (burn-in period) must be ignored (Orlande *et al.*, 2011; Ozisik and Orlande, 2000; Abreu *et al.*, 2014).

Before solving the inverse problem, the sensitivity coefficients must be analyzed. These coefficients have information about how the parameters estimations can be successfully made in the inverse step. The sensitivity coefficients are the elements of the sensitivity matrix and describe the relationship between temperature field and the parameter under analysis. In cases which the sensitivity coefficients have low magnitude values, a large change in parameters values will produce a small, or negligible, change in the temperature field, resulting in poor estimates. Besides that, to estimate more than one parameter simultaneously, the sensitivity coefficient of that parameter cannot be linearly dependent on others coefficients (Beck and Arnold, 1977; Orlande, 2012; Rojczyk *et al.*, 2017). In this work, the sensitivity coefficients $\mathbf{J}_{ij}$ will be computed numerically by applying a central finite difference scheme, defined in Eq. (35) (Beck and Arnold, 1977; Tannehill *et al.*, 1997).

$$\mathbf{J}_{ij} = \left[\frac{\partial {T_i}^T(\mathbf{P})}{\partial P_j}\right]^T \cong \frac{T_i(P_1, P_2, ..., P_j + \epsilon P_j, ..., P_N) - T_i(P_1, P_2, ..., P_j - \epsilon P_j, ..., P_N)}{2\epsilon P_j}. \tag{35}$$

In Eq. (35), $i = 1, 2, ..., D$, for which D is the number of time measures, and $j = 1, 2, ..., N$, for which N is the number of parameters. In this work, the reduced sensitivity coefficients will be examined. This quantity is computed multiplying $\mathbf{J}_{ij}$ by the parameter under analysis P_j seeking the qualitative examination of the linear dependence of the parameters.

5. RESULTS

The numerical code was implemented in Mathematica® considering the tissue as the human skin (65% of water and 35% of protein) with thermal properties indicated in Tab. 1 (Cooper and Trezek, 1971). Blood thermal properties, laser parameters settings and geometry dimensions are also presented in Tab. 1 (Abraham and Sparrow, 2007; Loiola *et al.*, 2018, 2020a). The value $\mu_{eff} = \mu_{eff}(exact)$ was assumed in the solution of the direct problem to generate simulated temperature measurements (Pearce *et al.*, 1994; Pearce, 2013). In simulations, the duration of the treatment (t_f) was kept maintaining a maximum temperature around 80 ^oC in the direct solution.

Table 1: Thermal properties and parameters applied in the verification phase.

Properties	Value	Unit	Properties	Value	Unit
ρ	1,140	kg/m^3	σ	0.5	mm
k	0.512	$W/m/K$	P	10	W
c_p	3,110	$J/kg/K$	T_∞	25	^oC
w_b	0.0028	$m_b^3/s/m_t^3$	h_∞	10	$W/m^2/K$
Q_m	170	W/m^3	R	3	mm
ρ_b	1,000	kg/m^3	H	3	mm
c_b	4,100	$J/kg/K$	t_f	0.0066	s
T_b	37	^oC	$\mu_{eff}(exact)$	4,060	m^{-1}

A comparison between the direct solution using the routine `NDSolve`, the software COMSOL Multiphysics® and the hybrid GITT approach to temperature variation is shown in Fig. 1. These solutions reveal an excellent agreement, with maximum difference between these results of nearly 0.05 ^oC. The GITT direct solution was solved with 200 eigenvalues and `NDSolve` was used to solve the system of coupled PDEs. This approach was applied in the sensitivity analysis and in the inverse solution presented below.

Figure 2 shows the reduced sensitivity coefficients as a time function in $r = 0$ and $z = H$ considering the values in Tab. 1 and the main parameters grouped as follows: $A = \rho c_p$, $B = k$, $C = \rho_b c_b w_b$, $D = Q_m$, $E = \mu_{eff}$ and $F = \sigma$. These groups are defined because some parameters does not appear independently in Eq. (1) and (7). In this figure we can observe the low magnitude values for the reduced sensitivity coefficients related to B, C and D parameters. The reduced sensitivity coefficients with respect to A, E and F have large magnitude values, but A and E are linearly dependent.

After this first sensitivity analysis, the sensitivity related to parameter μ_{eff} was observed in more detail. Figures 3a and 3b show the variation of $T(r, z, t)$ and $Q_l(r, z)$, respectively, for different values assumed for μ_{eff} considering $r = 0$ and $z = H$. The effective attenuation coefficient ranged from 3,020 m^{-1} to 5,980 m^{-1}, with an interval of 40 m^{-1}, and for each value it can be noted different temperature vs. time curves and different values for Q_l. Thus, μ_{eff} can be properly estimated in the inverse problem.

In the inverse analysis, the goal is to estimate the attenuation coefficient μ_{eff} considering two different values for the

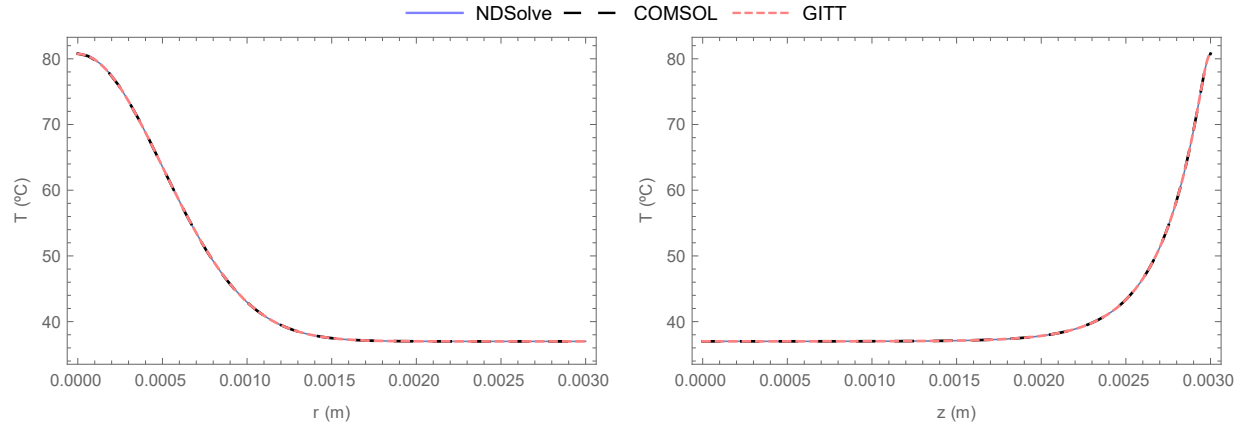

(a) Temperature variation in $t = t_f$ and $z = H$.

(b) Temperature variation in $t = t_f$ and $r = 0$.

Figure 1: Direct solution verification using different methods.

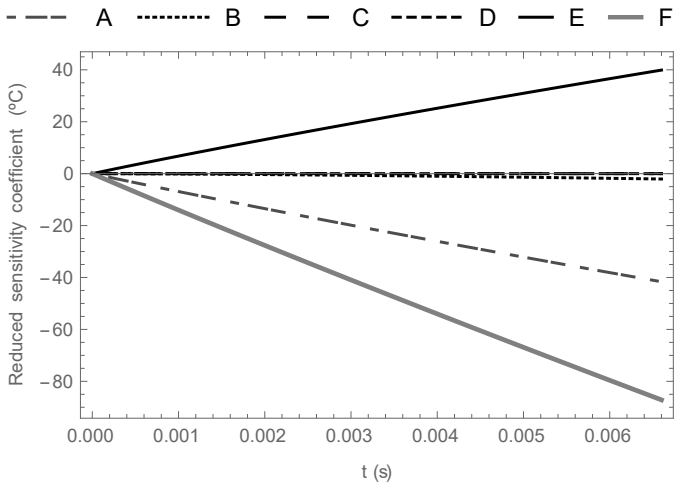

Figure 2: Sensitivity analysis in $r = 0$ and $z = H$.

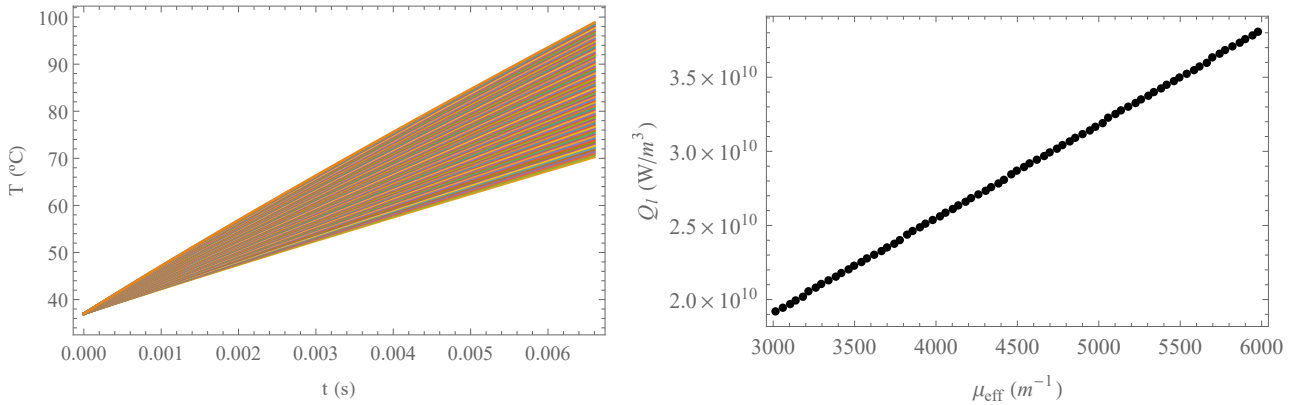

(a) Temperature vs. time.

(b) Laser heat source values.

Figure 3: Temperature variation and laser heat source at the heat surface considering different values of μ_{eff}.

laser power: $P = 10\ W$ and $P = 0.5\ W$. For this second value of laser power, the final time was extended to 0.2022 s and was assumed 75 eigenvalues in the direct solution. For the estimates, it was considered the measurements of the temperature at the heated surface and no prior information for μ_{eff}. The simulated measurements of temperature were obtained adding a Gaussian noise with zero mean and standard deviation of 0.05 C in the response provided by the direct problem and the candidate point was defined using a Gaussian proposal distribution with earlier accepted candidate as mean and standard deviation of 1 m^{-1}.

For $P = 10\ W$, the Markov chain was started with 50% of $\mu_{eff}(exact)$ and was simulated for 12,000 states with an acceptance rate of 63.7%, as illustrated in Fig. 4a. Figure 4b shows the states of the Markov chain between 5,500

and 12,000 and Fig. 4c shows the histogram of the marginal posterior distributions considering only these final states. Still considering this range, the mean was calculated and is obtained $\mu_{eff}(estimated) = 4059.53\ m^{-1}$, or the ratio $\mu_{eff}(estimated)/\mu_{eff}(exact) \approx 0.99988$, with a standard deviation of 1.17313 m^{-1} and a 99% credibility interval of $\{4056.87\text{-}4062.15\}\ m^{-1}$.

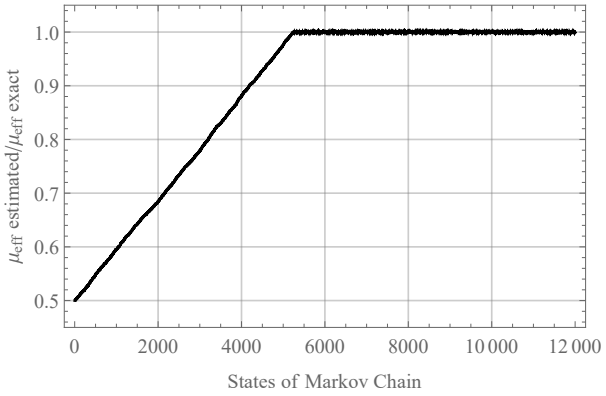

(a) Number of states.

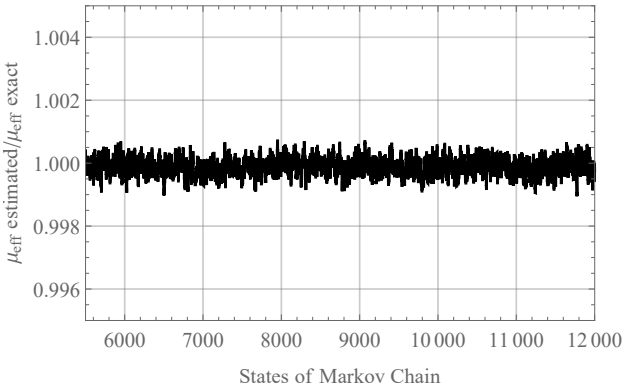

(b) States neglecting the burn-in period.

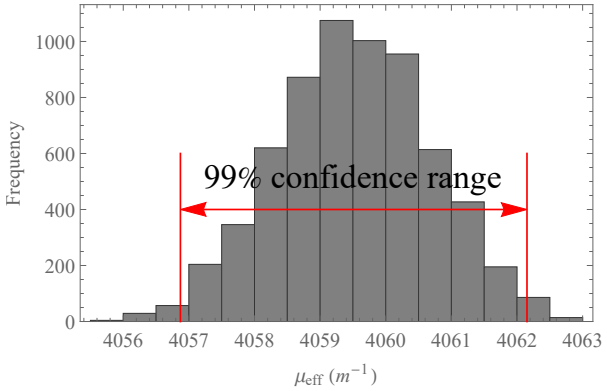

(c) Histogram.

Figure 4: Markov chain analysis for μ_{eff} and $P = 10\ W$.

Considering $P = 0.5\ W$, 80% of $\mu_{eff}(exact)$ was the value chosen to start the Markov chain which was simulated for 8,000 states with an acceptance rate of 71.5%, as shown in Fig. 5a. The states of the Markov chain between 2,500 and 8,000 is illustrated in Fig. 5b and Fig. 5c shows the histogram of the marginal posterior distributions considering these states. Then, a mean was calculated and $\mu_{eff}(estimated) = 4058.89\ m^{-1}$ defined, or $\mu_{eff}(estimated)/\mu_{eff}(exact) \approx 0.99973$, with 1.57976 m^{-1} as standard deviation and a 99% credibility interval of $\{4055.28\text{-}4062.62\}\ m^{-1}$.

A comparison of temperature vs. time curves was illustrated in Fig. 6a and Fig. 7a for $P = 10\ W$ and $P = 0.5\ W$, respectively, and the residuals, given by differences between the direct solutions considering $\mu_{eff}(estimated)$ and simulated measurements, was illustrated in Fig. 6b and Fig. 7b. The solutions using $\mu_{eff}(exact)$ and $\mu_{eff}(estimated)$ shows an excellent agreement for both values of laser power, and hence the inverse technique chosen are appropriate to estimate the desire parameter.

6. CONCLUSIONS

This research studied the estimation through an inverse approach of an optical parameter for a bioheat problem in which an external laser source heated a biological tissue. To achieve this goal, a methodology of solution applying the method GITT and the MCMC technique to solve the direct and inverse problem, respectively, was implemented in Mathematica® and was described in this paper. The direct solution was verified, against others numerical solutions, showing great agreement. In the inverse solution, simulated temperature measurements in the top surface of the tissue and two different values of laser power was considered. Optical properties are important parameters in thermal therapy when a laser is applied as a heat source and their values can vary from tissue to tissue and for the same tissue, depending on the environmental conditions. Therefore, the main contribution of this research is demonstrate a methodology that can be used to estimate accurately the effective attenuation coefficient and are able to quantify the uncertainties by applying the Bayesian framework.

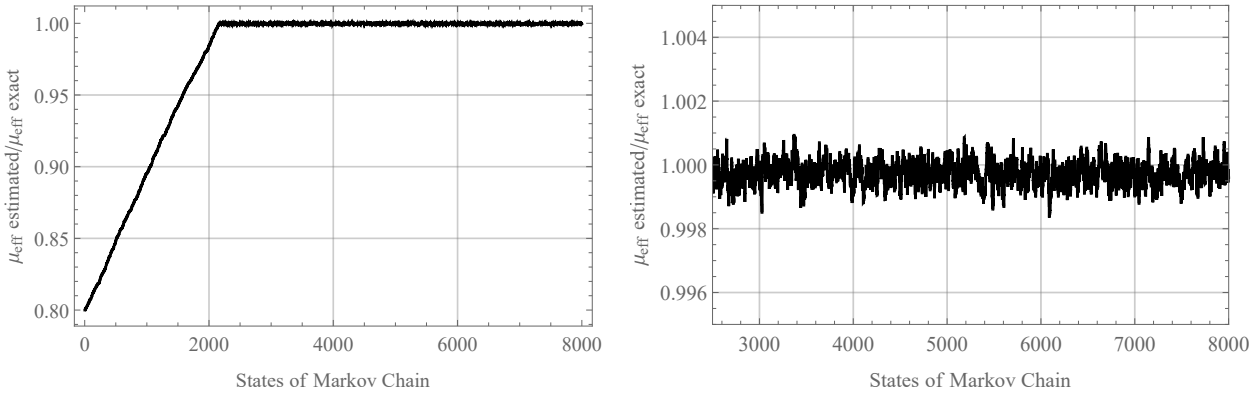

(a) Number of states.

(b) States neglecting the burn-in period.

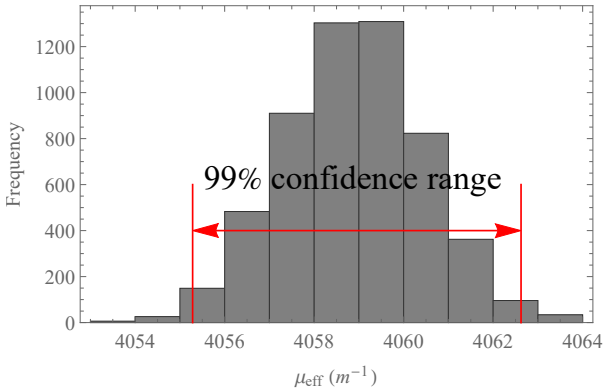

(c) Histogram.

Figure 5: Markov chain analysis for μ_{eff} and $P = 0.5\ W$.

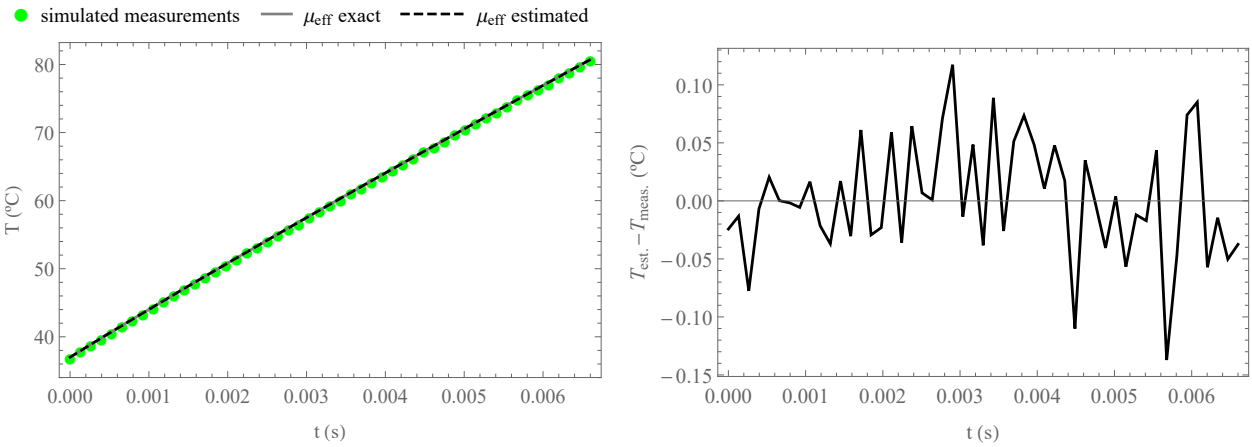

(a) Temperature vs. time curves for $\mu_{eff}(estimated)$ and $\mu_{eff}(exact)$.

(b) Residuals between solution for $\mu_{eff}(estimated)$ and simulated measurements.

Figure 6: Inverse solution analysis in $r = 0$ and $z = H$ for $P = 10\ W$.

7. ACKNOWLEDGEMENTS

This study was financed in part by the Coordenação de Aperfeiçoamento de Pessoal de Nível Superior - Brasil (CAPES) - Finance Code 001; and by Fundação Carlos Chagas Filho de Amparo à Pesquisa do Estado do Rio de Janeiro (FAPERJ).

8. REFERENCES

Abraham, J.P. and Sparrow, E.M., 2007. "A thermal-ablation bio-heat model including liquid-to-vapor phase change, pressure- and necrosis-dependent perfusion, and moisture-dependent properties". *International Journal of Heat and Mass Transfer*, Vol. 50, pp. 2537–2544.

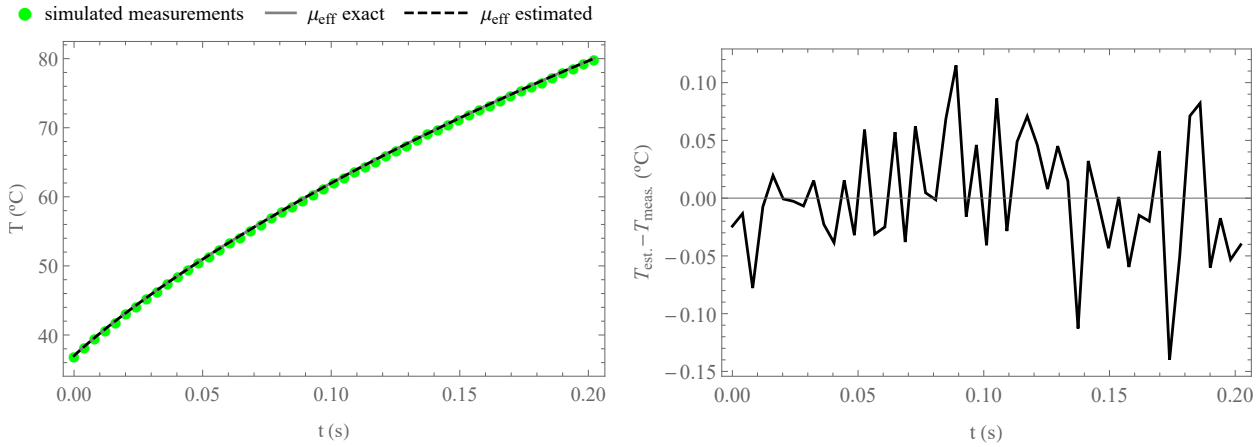

(a) Temperature vs. time curves for $\mu_{eff}(estimated)$ and $\mu_{eff}(exact)$.

(b) Residuals between solution for $\mu_{eff}(estimated)$ and simulated measurements.

Figure 7: Inverse solution analysis in $r = 0$ and $z = H$ for $P = 0.5\ W$.

Abreu, L.A., Orlande, H.R.B., Kaipio, J., Kolehmainen, V., Cotta, R.M. and Quaresma, J.N.N., 2014. "Identification of contact failures in multilayered composites with the markov chain monte carlo method". *Journal of Heat Transfer*, Vol. 136, pp. 101302/1–101302/9.

Beck, J.V. and Arnold, K.J., 1977. *Parameter estimation in engineering and science*. Wiley Interscience, New York.

Boyce, W.E. and DiPrima, R.C., 2000. *Elementary Differential Equations and Boundary Value Problems*. John Wiley & Sons, Inc, 7th edition.

Chato, J.C., 1992. "A view of the history of heat transfer in bioengineering". *Advances in Heat Transfer*, Vol. 22, pp. 1–18.

Cooper, T.E. and Trezek, G.J., 1971. "Correlation of thermal properties of some human tissues with water content". *Aerospace Medicine*, Vol. 42, No. 1, pp. 24–27.

Cotta, R.M., Knupp, D.C. and Quaresma, J.N.N., 2018. "Analytical methods in heat transfer". In *Kulacki, F. (eds) Handbook of Thermal Science and Engineering*. Springer, Cham, pp. 61–126.

Diller, K.R., 2010. "Laser generated heat transfer". In *Welch, A.J. and Van Gemert, M.J.C. (eds) Optical-thermal response of laser irradiated-tissue*. Springer, Dordrecht, pp. 353–397.

Habash, R.W.Y., Bansal, R., Krewski, D. and Alhafid, H.T., 2006. "Thermal therapy, part 1: An introduction to thermal therapy". *Critical reviews in biomedical engineering*, Vol. 34, pp. 459–479.

Jacques, S.L., Alter, C.A. and Prahl, S.A., 1987b. "Angular dependence of HeNe laser light scattering by human dermis". *Lasers in the Life Sciences*, Vol. 1, pp. 309–333.

Jacques, S.L. and Prahl, S.A., 1987a. "Modeling optical and thermal distributions in tissue during laser irradiation". *Lasers in Surgery and Medicine*, Vol. 6, No. 6, pp. 494–503.

Kaipio, J. and Somersalo, E., 2004. *Statistical and Computational Inverse Problems, Applied Mathematical Sciences*, Vol. 160. Springer-Verlag New York, New York.

Kim, A. and Wilson, B.C., 2010. "Measurement of ex vivo and in vivo tissue optical properties: Methods and theories". In *Welch, A.J. and Van Gemert, M.J.C. (eds) Optical-thermal response of laser irradiated-tissue*. Springer, Dordrecht, pp. 267–319.

Loiola, B.R., Abreu, L.A. and Orlande, H.R.B., 2020b. "Thermal characterization of ex vivo tissue". *Critical Reviews in Biomedical Engineering*, Vol. 48, pp. 111–124.

Loiola, B.R., Orlande, H.R.B. and Dulikravich, G.S., 2018. "Thermal damage during ablation of biological tissues". *Numerical Heat Transfer Applications*, Vol. 73, pp. 685–701.

Loiola, B.R., Orlande, H.R.B. and Dulikravich, G.S., 2020a. "Approximate Bayesian computation applied to the identification of thermal damage of biological tissues due to laser irradiation". *International Journal of Thermal Sciences*, Vol. 151, pp. 106243/1–106243/13.

Nicolaides, L., Chen, Y., Mandelis, A. and Vitkin, I.A., 2001. "Theoretical, experimental, and computational aspects of optical property determination of turbid media by using frequency-domain laser infrared photothermal radiometry". *Optical Society of America*, Vol. 18, No. 10, pp. 2548–2556.

Orlande, H.R.B., 2012. "Inverse problems in heat transfer: New trends on solution methodologies and applications". *Journal of Heat Transfer*, Vol. 134, pp. 031011/1–031011/13.

Orlande, H.R.B., Colaço, M.J., Cotta, C.P.N., Guimarães, G. and Borges, V.L., 2011. *Problemas Inversos em Transferência de Calor*, Vol. 51. Notas em Matemática Aplicada. SBMAC - Sociedade Brasileira de Matemática Aplicada e

Computacional, São Carlos (SP).

Ozisik, M.N., 1993. *Heat Conduction*. Wiley Interscience, New York (NY), 2nd edition.

Ozisik, M.N. and Orlande, H.R.B., 2000. *Inverse Heat Transfer: Fundamentals and Applications*. Taylor & Francis, 1st edition.

Pearce, J.A., 2013. "Comparative analysis of mathematical models of cell death and thermal damage process". *International Journal of Hyperthermia*, Vol. 29, No. 4, pp. 262–280.

Pearce, J.A., Çilesiz, I., Welch, A.J., Chan, E., McMurray, T.J. and Thomsen, S., 1994. "Comparison of Ho:YAG, Tm:YAG and argon lasers for fusion of intestinal tissues". *Proc. SPIE Laser Surgery: Advanced Characterization, Therapeutics, and Systems IV*, Vol. 2128, pp. 517–526.

Pennes, H.H., 1948. "Analysis of tissue arterial blood temperature in the resting forearm". *Journal of Applied Physiology*, Vol. 1, No. 2, pp. 93–122.

Prahl, S.A., Vitkin, I.A., Bruggemann, U., Wilson, B.C. and Anderson, R.R., 1992. "Determination of optical properties of turbid media using pulsed photothermal radiometry". *Physics in Medicine and Biology*, Vol. 37, No. 6, pp. 1203–1217.

Rojczyk, M.J., Orlande, H.R.B., Colaço, M.J., Szczygiel, I., Nowak, A.J., Bialecki, R.A. and Ostrowski, Z., 2017. "Inverse heat transfer problems: an application to bioheat transfer". *Computer Assisted Methods in Engineering and Science*, Vol. 22, pp. 365–383.

Tannehill, J.C., Anderson, D.A. and Pletcher, R.H., 1997. *Computational fluid mechanics and heat transfer: series in computational and physical processes in mechanics and thermal sciences*. Taylor&Francis, 2nd edition.

Welch, A.J., 1984. "The thermal response of laser irradiated tissue". *IEEE Journal of Quantum Electronics*, Vol. 20, No. 12, pp. 1471–1481.

Welch, A.J., van Gemert, M.J.C. and Star, W.M., 2010. "Definitions and overview of tissue optics". In *Welch, A.J. and Van Gemert, M.J.C. (eds) Optical-thermal response of laser irradiated-tissue*. Springer, Dordrecht, pp. 27–64.

Wolfram, 2020. "Wolfram Language & System: Documentation Center". <https://reference.wolfram.com/language/?source=nav>. Access: 14 Sep. 2020.

9. RESPONSIBILITY NOTICE

The authors are solely responsible for the printed material included in this paper.